Excerpt from the Proceedings of the 2011 COMSOL Conference in Boston

Computational Acoustic Attenuation Performance of Helicoidal Resonators Comparable to Experiment

Wojciech ŁAPKA*
Division of Vibroacoustics and Systems Biodynamics, Institute of Applied Mechanics,
Poznań University of Technology, Poland.
*Corresponding author: W. Łapka, Piotrowo 3 Street, 60-965 Poznań, Poland. wojciech.lapka@put.poznan.pl

Abstract: This paper concerns to the problem of obtaining proper acoustic attenuation performance by making computations, which are comparable to the experimental results, when modeling helicoidal resonators. It was observed that modeling acoustic systems with helicoidal resonators in COMSOL Multiphysics don't need to include all of experimentally used environment to achieve similar results, but the boundary conditions should be properly used. There are presented examples of different acoustic systems with helicoidal resonators and acoustic attenuation performance parameters numerically computed compared with insertion loss measured experimentally.

Keywords: helicoidal resonator, sound attenuation, experiment, computation.

1. Introduction

The research work carried out on the solution called helicoidal resonator [2-5] or as before "spiral ducts" [6-11] gave thoughts on the conditions to be met by numerical simulations which are comparable to experiment. This was due to the necessity to carry out several simulations, assuming different boundary conditions, or because of having to change the numerical model in order to obtain relevant results. It was observed that modeling acoustic systems with helicoidal resonators in COMSOL Multiphysics [1] don't need to include all of experimentally used environment to achieve similar results, but the boundary conditions should be properly used.

2. Numerical research characteristics

2.1 Use of COMSOL Multiphysics

Numerical computations were realized by the use of COMSOL Multiphysics - Acoustic Module [1]. Finite Element Method (FEM) was used to solve three-dimensional (3D) numerical models in the frequency domain by the use of time-harmonic Pressure Acoustics application.

The final solving parameter is the acoustic pressure p [Pa], which can be computed by the use of slightly modified Helmholtz equation:

$$\nabla \cdot \left(-\frac{\nabla p}{\rho_0} \right) - \frac{\omega^2 p}{c_s^2 \rho_0} = 0 \qquad (1)$$

where ρ_0 is the density of air (ρ_0=1,23 kg/m^3), c_s is the speed of sound in air (c_s=343m/s), and ω gives the angular frequency.

2.2 Boundary conditions

For investigated models in this work the boundary conditions are of four types [1]. For acoustically hard walls at the solid boundaries, which are the walls of the helicoidal profile, mandrel and cylindrical duct, the model uses sound hard (wall) boundary conditions:

$$\left(\frac{\nabla p}{\rho_0} \right) \cdot \mathbf{n} = 0 \qquad (2)$$

First type of the inlet boundary condition (sound source) of cylindrical duct used in this research is a combination of incoming and outgoing plane waves, as follows:

$$\mathbf{n} \cdot \frac{1}{\rho_0} \nabla p + ik \frac{p}{\rho_0} + \frac{i}{2k} \Delta_T p = \\ = \left(\frac{i}{2k} \Delta_T p_0 + \left(1 - (\mathbf{k} \cdot \mathbf{n})\right) ik \frac{p_0}{\rho_0} \right) e^{-ik(\mathbf{k} \cdot \mathbf{r})} \qquad (3)$$

Here Δ_T denotes the boundary tangential Laplace operator, $k=\omega/c_s$ is the wave number, r is the shortest distance from the point $\mathbf{r}=(x,y,z)$ on the boundary to the source , $\mathbf{n}$ is the normal direction vector for investigated cylindrical duct, and wave vector is defined as $\mathbf{k}=k\mathbf{n}_\mathbf{k}$, where $\mathbf{n}_\mathbf{k}$ is the wave-direction vector, p_0 represents the applied outer pressure, and i denotes the imaginary unit. The inlet boundary condition is valid as long as the frequency is kept below the cutoff frequency for

the second propagating mode in the cylindrical duct [1].

Second type of the inlet boundary condition (sound source) of cylindrical duct is radiation condition of a spherical wave with an incoming plane wave included [1], as follows:

$$\mathbf{n}\cdot\left(\frac{1}{\rho_0}(\nabla p-\mathbf{q})\right)+\left(ik+\frac{1}{r}\right)\frac{p}{\rho_0}-\frac{r\Delta_T p}{2\rho_0(ikr+1)}= \\ =\left(\frac{-r\Delta_T p}{2\rho_0(ikr+1)}+\left(ik+\frac{1}{r}-i\mathbf{k}\cdot\mathbf{n}\right)\frac{p_0}{\rho_0}\right)e^{-i\mathbf{k}\cdot\mathbf{r}} \quad (4)$$

which emanates from inlet circular boundary and allows a radiated wave to leave the modeling domain without reflections.

For the outlet boundary is also used the radiation boundary condition which allows an outgoing wave to leave the modeling domain with no or minimal reflections:

$$\mathbf{n}\cdot\frac{1}{\rho_0}\nabla p+i\frac{k}{\rho_0}p+\frac{i}{2k}\Delta_T p=0 \quad (5)$$

2.3 Numerical models

The numerical models are computed by the use of finite element method by the terms of the element size [12]. Therefore, the maximum element size equals h_e=0,2(c_s/f_{max}), where f_{max} is the value of maximum investigated frequency (in this paper f_{max}=1600Hz).

Three dimensional numerical model of acoustic system (Fig. 1), which consists: a) cylindrical duct with boundary conditions at the inlet and outlet compatible with equations (3) and (4) (these boundary conditions make cylindrical duct as infinite long), and b) helicoidal resonator placed inside this duct, were used to achieve transmission loss in computations.

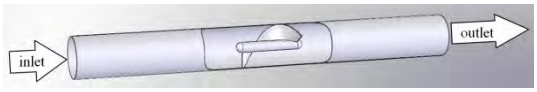

Figure 1. Schematic view of acoustic system with helicoidal resonator to obtain transmission loss computationally.

However, in order to obtain the insertion loss through numerical calculations a model was built consisting of a cylindrical duct with a length of 100cm (where helicoidal resonators were placed in the same distance from the beginning of the duct as presented in Fig. 5) and on its outlet side of the cube of 100cm, in which all the walls was assumed the boundary condition of a characteristic impedance of air ($\rho_0 c_s$).

Here at the inlet boundary was used radiation condition of a spherical wave (4) with an incoming plane wave included.

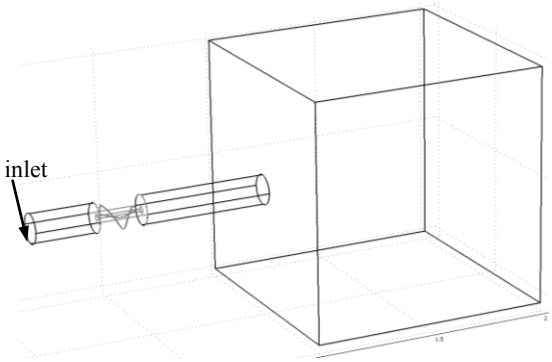

Figure 2. Schematic view of acoustic system with helicoidal resonator for computation of the insertion loss in COMSOL program.

Also different kind of configurations of boundary conditions use will be considered in a results part of this work.

3. Experimental research characteristics

The acoustical measurements of insertion loss were carried out for two helicoidal resonators with two number of turns ***n*=0,671** and ***n*=0,695**, and following other parameters: relation between one helicoidal turn s and diameter of cylindrical duct d, ratio ***s/d*=1,976**; relation between diameter of mandrel d_m and d, ratio ***d_m/d*=0,24**, relation between thickness of helicoidal profile g and d, ratio ***g/d*=0,024**, placed inside cylindrical duct of diameter d=12,5cm and length l=100cm. Basic dimensions of helicoidal resonator are presented in Fig. 3.

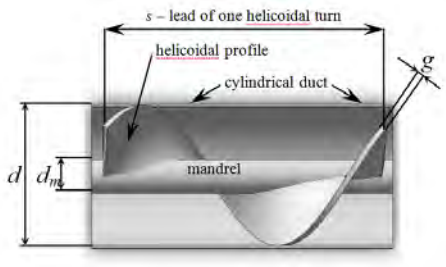

Figure 3. Basic dimensions of helicoidal resonator.

Source signal was the white noise. Both helicoidal resonators were made by the use of a three dimensional rapid prototyping technique SLS. Thus, the shape of resonators is exactly the same as in the simulation. To measure sound pressure levels at the outlet of cylindrical ducts were used Brüel & Kjær's platform PULSE for noise and vibration analysis equipped with Brüel & Kjær's 1/2 inch acoustical microphone type 4190-C-001.

Experimental researches were carried out in Vibroacoustic Laboratory of Poznań University of Technology at the laboratory test set up as shown in Fig. 4, made in the years 2008-2009 during realizing the promotional research project of the Polish Ministry of Science and Higher Education.

Figure 4. Example view on the experimental set up.

The experimental set up is specially designed to measure cylindrical ducts with diameter d=12,5cm by inserting them tightly to acoustical source tube orifice.

Distance between inlet of the pipe and a broadband speaker equals 16cm. The external dimensions of an acoustic source tube are 33cm in diameter and 48cm in length. The source tube is filled inside with an absorptive material - polyurethane foam.

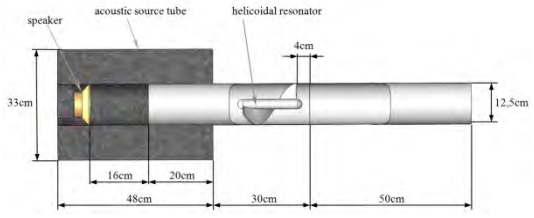

Figure 5. Schematic view of the experimental set up in the laboratory experiment.

As it is shown in Fig. 5 the distance between one end of the helicoidal profile and cross sectional plane in the middle of the cylindrical duct was 4cm in both cases - experimental and numerical.

4. Acoustic attenuation performance parameters

Two types of acoustic attenuation performance parameters are used in this work [13]:

1) Transmission Loss (TL), used only in computations, given by:

$$TL = 10 \cdot \log_{10}\left[\frac{\frac{p_0^2}{2\rho_0 c_s}}{\frac{|p_2|^2}{2\rho_0 c_s}}\right], \quad [dB] \tag{6}$$

where p_0 denotes maximum amplitude of source sound pressure at the inlet [Pa], p_2 denotes maximum amplitude of sound pressure at the outlet [Pa], and $\rho_0 c_s$ is the characteristic impedance of air.

2) Insertion Loss (IL), used both in computations and experiment, given by:

$$IL = SPL_1 - SPL_2, \ [dB] \tag{7}$$

where SPL_1 denotes the sound pressure level at the outlet of cylindrical duct without filter, [dB], and SPL_2 denotes the sound pressure level at the outlet of cylindrical duct with filter, [dB].

5. Results

In case of experimental results that are represented only by insertion loss (IL), the research made by the use of numerical calculations in COMSOL Multiphysics are focused on achieving the best convergence. The insertion losses were achieved by calculating all models twice, with and without helicoidal resonators.

Acoustic experimental model, schematically presented in Fig. 5, can be represented in first approach by numerical model 1 (NM1) as presented in Fig. 6. It consists 1,16m long pipe, which is surrounded at the inlet side in the distance of 16cm by an absorptive material (close to polyurethane foam) of apparent density 150kg/m^3 and 8e-6m of mean fiber diameter when used Delany and Bazley type of subdomain damping in COMSOL [1]. At the end of model 1 is situated 1m cubic box with

characteristic impedance of air as a boundary condition on its all walls.

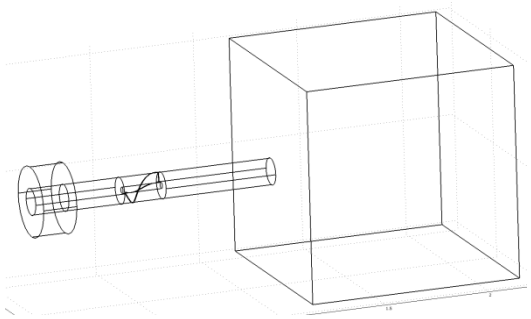

Figure 6. Numerical model 1 (NM1) - 1,16m long pipe with helicoidal resonator surrounded at the inlet side in the distance of 16cm by an absorptive material.

In Fig. 7 is presented comparison between experimental IL and achieved on the base of numerical calculations NM1 IL with two types of inlet boundary conditions, plane wave and spherical wave.

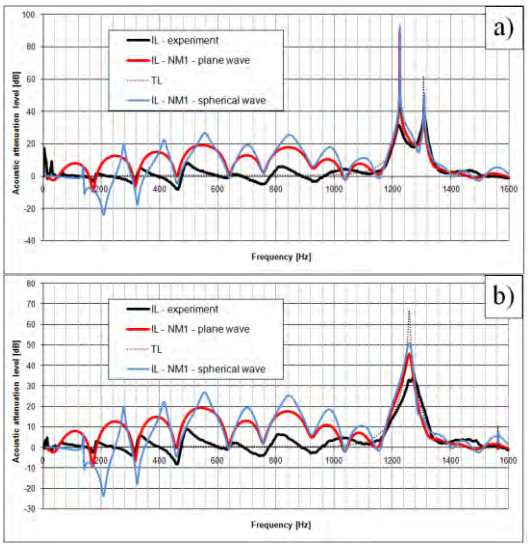

Figure 7. Comparison of results for NM1 for helicoidal resonators with number of turns: a) n=0,671, b) n=0,695.

Second case is numerical model 2 (NM2) which consists 1,16m long pipe, helicoidal resonator and 1m cubic box at the outlet, as presented in Fig. 8. NM2 differs from NM1 only by excluding surrounding absorptive material at the distance of 16cm at the inlet part of the pipe.

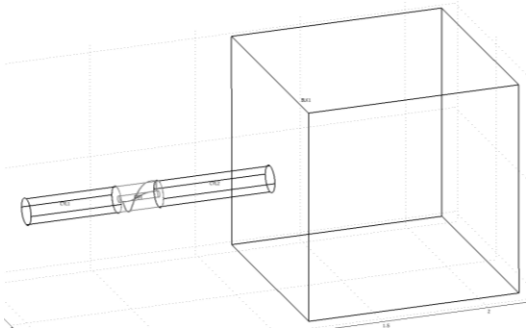

Figure 8. Numerical model 2 (NM2) - 1,16m long pipe with helicoidal resonator and 1m cubic box.

In Fig. 9 is presented comparison between experimental IL and achieved on the base of numerical calculations NM2 IL with two types of inlet boundary conditions, plane wave and spherical wave.

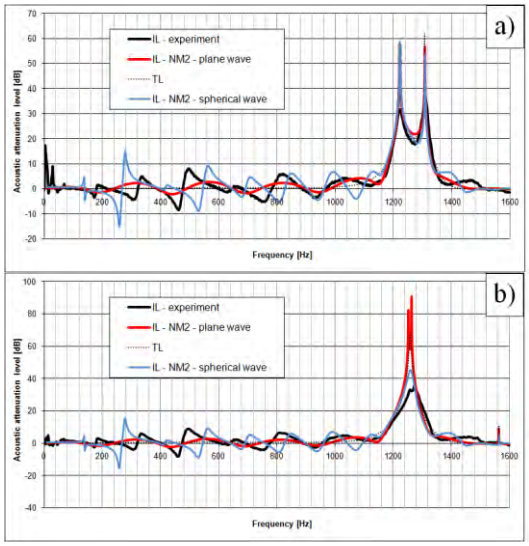

Figure 9. Comparison of results for NM2 for helicoidal resonators with number of turns: a) n=0,671, b) n=0,695.

Third case is numerical model 3 (NM3) which consists 1m long pipe, helicoidal resonator and 1m cubic box at the outlet, as presented in Fig. 10. NM3 differs from NM2 only by cutting the pipe from 1,16m to 1m.

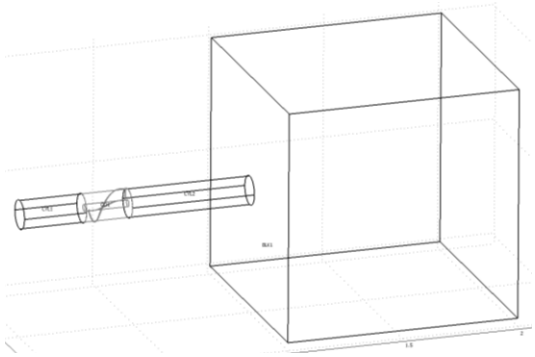

Figure 10. Numerical model 3 (NM3) - 1m long pipe with helicoidal resonator and 1m cubic box.

In Fig. 11 is presented comparison between experimental IL and achieved on the base of numerical calculations NM3 IL with two types of inlet boundary conditions, plane wave and spherical wave.

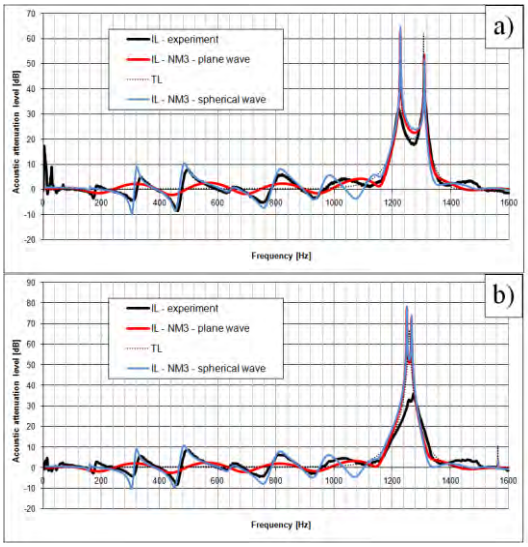

Figure 11. Comparison of results for NM3 for helicoidal resonators with number of turns: a) n=0,671, b) n=0,695.

6. Conclusions

This work presents the study of achieving best convergence between experimental and numerical results of modeling acoustics systems with helicoidal resonators. However, this study can be very helpful during considerations of any ducted acoustic systems, where the comparison between experimental and numerical results is desirable.

As it can be observed from presented results, the best convergence between experimental and numerical ILs is achieved by modeling just 1m long pipe with helicoidal resonator inside and inlet boundary condition set as spherical wave. This numerical acoustic system differs a lot from experimental set up.

It was also observed that in all cases of numerical models (from NM1 to NM3) the characteristic for presented helicoidal resonators sound attenuation frequency range between about 1150Hz to about 1340Hz can be simply identified. But the conditions play a key role when identifying lower frequency range of acoustic characteristics.

This study shows that modeling acoustic systems with helicoidal resonators in COMSOL Multiphysics don't need to include all of experimentally used environment to achieve similar results, but the boundary conditions should be properly used. Also it is a great knowledge to know which exact numerical model should be used to achieve results comparable to experiment.

7. References

1. COMSOL Multiphysics version 3.4, *Acoustic Module, User's Guide and Model Library Documentation Set*, COMSOL AB, www.comsol.com, Stockholm, Sweden, (2007)
2. Łapka W., Acoustic attenuation performance of helicoidal resonator due to distance change from different cross-sectional elements of cylindrical ducts, *Proceedings of the European COMSOL Conference 2010*, ISBN: 978-0-9825697-7-1, 17-19 November 2010, Paris, France, 7 (2010)
3. Łapka W., Acoustical properties of helicoid as an element of silencers, *PhD Thesis*, Poznań University of Technology, Faculty of Mechanical Engineering and Management, Poznań, Poland, 121 (2009)
4. Łapka W., Helicoidal resonator, *Proceedings of the 39th International Congress on Noise Control Engineering*, Inter-Noise 2010, 13-16 June 2010, Lisbon, Portugal, 9 (2010)
5. Łapka W., Influence of change of mandrel diameter of helicoidal resonator on its acoustic attenuation performance, *Proceedings of the 57th Open Seminar on Acoustics - OSA 2010,* ISBN 978-83-931744-0-9, 20-24 September 2010, Gliwice, Poland, 121-124 (2010)

6. Łapka W., Sound propagation through circular ducts with spiral element inside, *Proceedings of the European COMSOL Conference 2008*, 4-6 November 2008, Hannover, Germany, 5 (2008)
7. Łapka W., Insertion loss of spiral ducts - measurements and computations, *Archives of Acoustics*, **34**, No 4, 537-545, (2009)
8. Łapka W., Cempel C., Computational and experimental investigations of a sound pressure level distribution at the outlet of the spiral duct, *Archives of Acoustics*, **33**, No. 4 (Supplement), 65-70, (2008)
9. Łapka W., Cempel C., Acoustic attenuation performance of Helmholtz resonator and spiral duct, *Vibrations in Physical Systems*, **23**, 247-252, (2008)
10. Łapka W., Acoustic attenuation performance of a round silencer with the spiral duct at the inlet, *Archives of Acoustics*, **32**, No 4 (Supplement), 247-252, (2007)
11. Łapka W., Cempel C., Noise reduction of spiral ducts, *International Journal of Occupational Safety and Ergonomics (JOSE),* **13**, No. 4, 419-426, (2007)
12. Marburg S., Nolte B., *Computational Acoustics of Noise Propagation in Fluids – Finite and Boundary Element Methods*, Springer-Verlag, Berlin, Germany, 578 (2008)
13. Munjal M. L., *Acoustics of Ducts and Mufflers with Application to Exhaust and Ventilation System Design*, Inc., Calgary, Canada, John Wiley & Sons, 328 (1987)

8. Acknowledgements

Scientific work financed from the budget for science in the years 2010-2013 as a research project.